

INR ACTIVITY IN THE ACCELERATING CAVITIES DEVELOPMENT AND STUDY FOR ILC POSITRON SOURCE PARAMETERS

*V. V. Paramonov¹, L. V. Kravchuk, V. A. Moiseev, A. N. Naboka,
A. K. Skasyrskaya*

Institute for Nuclear Research RAS, Moscow

The critical part of the Normal Conducting (NC) Positron Pre-Accelerator (PPA) in ILC Positron Source (PS) is capture sections, which should operate with an accelerating gradient of up to 15 MV/m in combination with long RF pulse (~ 1 ms). Developed in INR and now constructing in DESY, the CDS booster cavity for the Photo Injector Test facility, DESY, Zeuthen, will operate at the same conditions and is a full-scale, high RF power prototype of the PS capture cavities. Cavity construction status and results of the cavity tuning at low RF level are presented. Another features of the standing wave cavities for PPA, such as RF pulsed heating, advanced cooling and beam loading are discussed.

Критичной частью нормально проводящего предускорителя позитронов в источнике позитронов ILC являются секции захвата, которые должны работать с темпом ускорения до 15 МВ/м в сочетании с длинным, до 1 мс, ВЧ-импульсом. Разработанный в ИЯИ РАН и сооружаемый в DESY бустерный резонатор для стенда исследования ВЧ-фотоинжекторов в DESY (Цойтен) будет работать в аналогичных условиях и являться полномасштабным прототипом на высоком уровне ВЧ-мощности для секций захвата источника позитронов. Приводится описание изготовления резонатора и результаты настройки на низком уровне ВЧ-мощности. Рассматриваются другие особенности резонаторов для предускорителя, такие как нагрузка пучком, импульсный ВЧ-нагрев, усовершенствованное охлаждение.

PACS: 29.20.-c; 29.25.-t

INTRODUCTION

In the future ILC main linacs will be constructed with superconducting accelerating cavities. But, in the indispensable ILC part — undulator-based Positron Source PPA, the NC structures should be used. Proposal of the Standing Wave (SW) PPA, based on NC compensated CDS structure, has been developed [1] before. Main features of this proposal remain relevant in present ILC PS PPA conceptual design [2], in which Traveling Wave (TW) structures are assumed.

SW operating mode for PPA was selected in [1] due to noticeably higher total RF efficiency [3] and compensated CDS [4] structure was applied basing on well-known world-wide experience — such structures combine high RF efficiency with parameters stability and operational reliability. Anyhow, PPA capture sections will operate in SW mode, in combination

¹E-mail: paramono@inr.ru

of strong fields, long RF pulse and heavy average heat loading. ILC bunch parameters lead to specific beam loading effect in accelerating structure. Results of INR activity in these features study are briefly considered in the report.

1. CDS BOOSTER CAVITY FOR PITZ

The Booster Cavity (BC) layout is shown in Fig.1 and general parameters are listed in Table. In more detail the cavity design is described in [5].

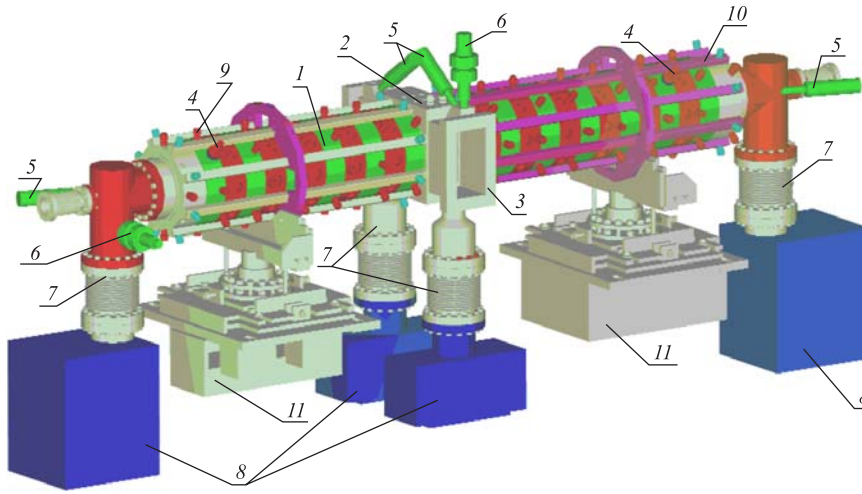


Fig. 1. Booster cavity layout. 1 — regular cells; 2 — RF coupler; 3 — RF flanges; 4 — RF probes; 5 — photomultipliers; 6 — vacuum gauges; 7 — pumping ports; 8 — ion pumps; 9 — internal cooling circuit; 10 — outer cooling circuit; 11 — support and adjustment

As one can see from Table, in main operational parameters BC complies to ILC PPA capture sections requirements [6]. For main PPA part accelerating structure will operate with more soft regime, accelerating gradient ~ 8.5 MV/m, and high power test under capture section parameters will also answer for structure reliability in all PPA parts.

1.1. Cavity Construction Status. BC is now under construction in DESY, Hamburg. Extensive low RF level test program has been performed to investigate cells production results, to verify RF tuning procedure, brazing procedure and cells parameters change after brazing. Results of the test program have shown very narrow cell frequencies spread, $\approx 3 \cdot 10^{-5} f_0$ for accelerating and $\approx 1.5 \cdot 10^{-4} f_0$ for coupling mode frequencies.

PITZ-2 BC parameters

Parameter	Value
Operating frequency, MHz	1300
Nominal gradient $E_0 T$, MV/m	12.5
Maximal gradient $E_0 T$, MV/m	14.0
Maximal surface field, MV/m	40.0
Maximal RF pulse power, MW	8.6
Maximal RF pulse length, μs	900
Nominal repetition rate, Hz	5
Aperture diameter, mm	30.0
Group velocity, % c	5.6

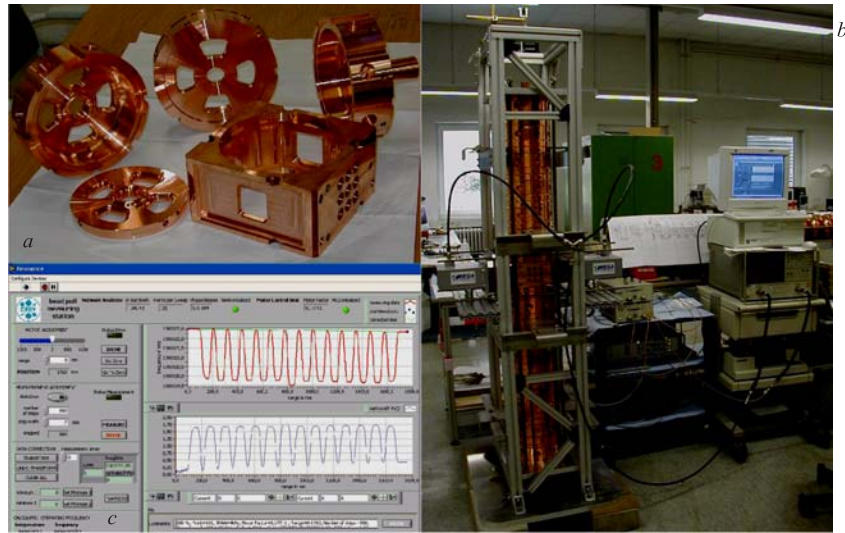


Fig. 2. Booster cavity components, specimens (a), cavity assembly for low-level RF tuning (b) and electric field distribution along axis (c)

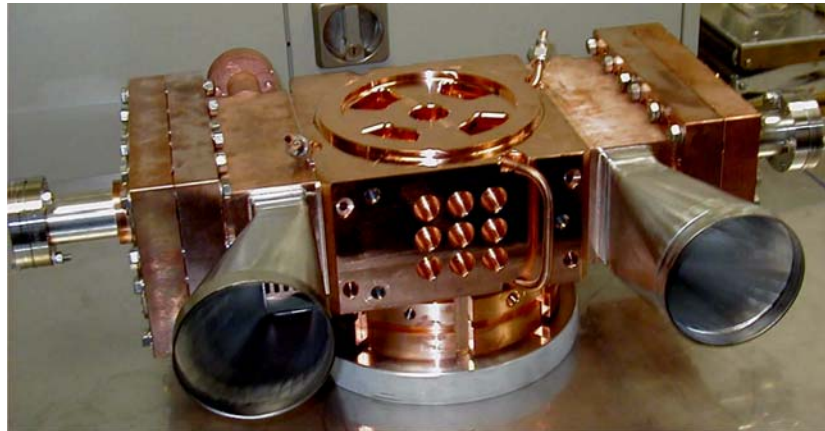


Fig. 3. Brazed BC coupler cell

All cavity components, specimens shown in Fig. 2, a, are produced in industry. Tuning procedure has been established, Fig. 2, b. Both operating and coupling mode frequencies were adjusted to target values for total cavity assembly, without individual cells tuning. Electric field distribution along the cavity axis, shown in Fig. 2, c for preliminary tuned cavity, confirms compensated structures advantage — high stability with respect to cells parameters deviations. Cavity RF tuning before brazing is completed. Multi-step brazing procedure in vacuum is adopted for cavity construction. The RF coupler cell, brazed with connecting flanges and adjacent regular half-cell, is shown in Fig. 3. Symmetrical RF coupler, with two input windows, is developed for the cavity.

2. RF PULSED HEATING

CDS structures for ILC PPA are described in [6] both in high, $E_0T \approx 15$ MV/m, and in moderate (≈ 8.5 MV/m) accelerating gradient options. For high gradient CDS operation the maximal magnetic field $H_{s \max} \sim 60$ kA/m at the end of coupling windows will be realized, resulting in power pulse loss density $P_{d \max} = 1.55 \cdot 10^7$ W/m². These are not so small, for pulsed heating effect, values. RF pulsed heating effect particularities in NC L-band cavities are considered in [8]. In cavities, operating in combination of strong fields and long RF pulse the effect becomes apparent mainly due to long RF pulse and consists in cavity parameters change during RF pulse. During RF pulse time $\tau \sim 1$ ms heat penetrates into cavity at depth ~ 240 μ m. Surface temperature rise T_s distribution repeats well the pulse RF loss density one. Maximal T_s value can be significant and leads to measurable quality factor reduction during RF pulse. For constant input RF power it results in field decreasing during the pulse. Expansion of thin heated layer at the cavity surface leads to cavity deformation and to cavity frequency change δf . Pulse cavity deformations are elastic.

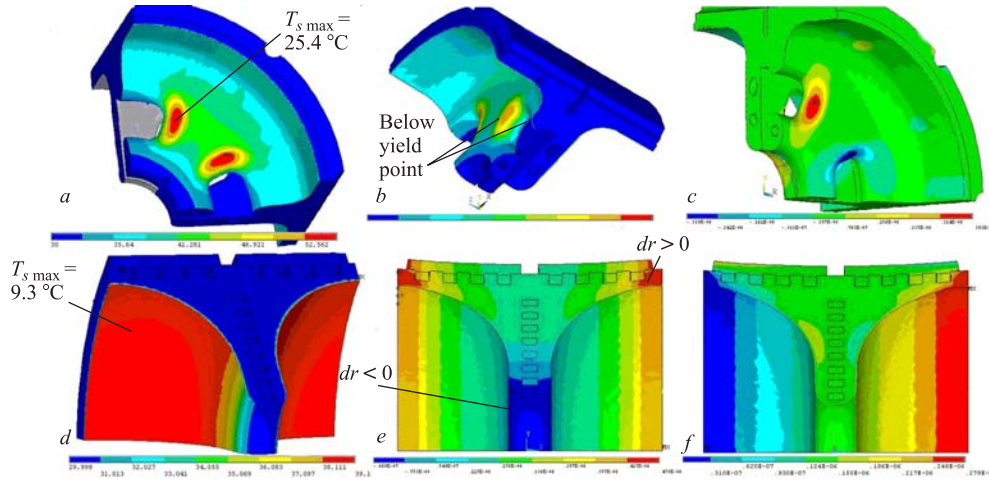


Fig. 4. Pulsed temperature (a), stress (b) and displacements (c) distributions after $\tau = 1$ ms RF pulse, $E_0T = 15$ MV/m in CDS for PPA in comparison with temperature (d), radial (e) and longitudinal (f) displacements distributions in simple π -structure [7]

Pulsed RF heating effect in CDS PPA options is considered in [8] and compared with the same effect in simple π -structure [7], proposed for the same purpose. Surface temperature rise and displacements distribution are shown in Fig. 4 for both structures. Instead of higher local temperature rise in CDS PPA, Fig. 4, a, an effect summary for both structures is the same — maximal displacements value ~ 1 μ m, frequency shift ~ 4 kHz for CDS and ~ -4 kHz for simple π -structure, quality factor degradation $\sim 1\%$ during 1 ms RF pulse. Pulsed RF heating effects both in CDS PPA, and in simple π -structure are several times less, as compared to operating DESY RF gun cavities [8].

3. ADVANCED COOLING SIMULATIONS

An average heat loading in CDS BC and CDS PPA is ~ 25 kW/m. Cooling CDS capability, taking into account real RF losses distribution, has been considered in two approaches. In engineering approach a prescribed heat exchange coefficient value at the cooling channels surface, estimated from approximate semi-empirical relations, is usually used. In conjugated approach we start from turbulent flow parameters simulation in cooling channels. At the second step we solve self-consistent heat exchange problem cavity body — cooling fluid.

Conjugated approach is more logical, because it takes into account cooling fluid temperature rise in passing through cooling channel and can take into account material and fluid parameters change with temperature. This approach is very useful for cooling problem simulations for cavities with very high heat load, providing detailed temperature distribution picture. Indubitable value of this approach is in possibility of flow distribution estimation in complicated cooling circuit and detailed cooling ability study for each part. But this approach is much more resource consuming, as compared to the engineering one.

Temperature distributions in CDS BC cell, calculated in engineering and conjugated approaches, are shown in Fig. 5. One can see in Fig. 5, *b* cooling water temperature change along cooling channels. Heat load both in BC and in PPA CDS is not extremely high and results of cooling simulations in two approaches are very close.

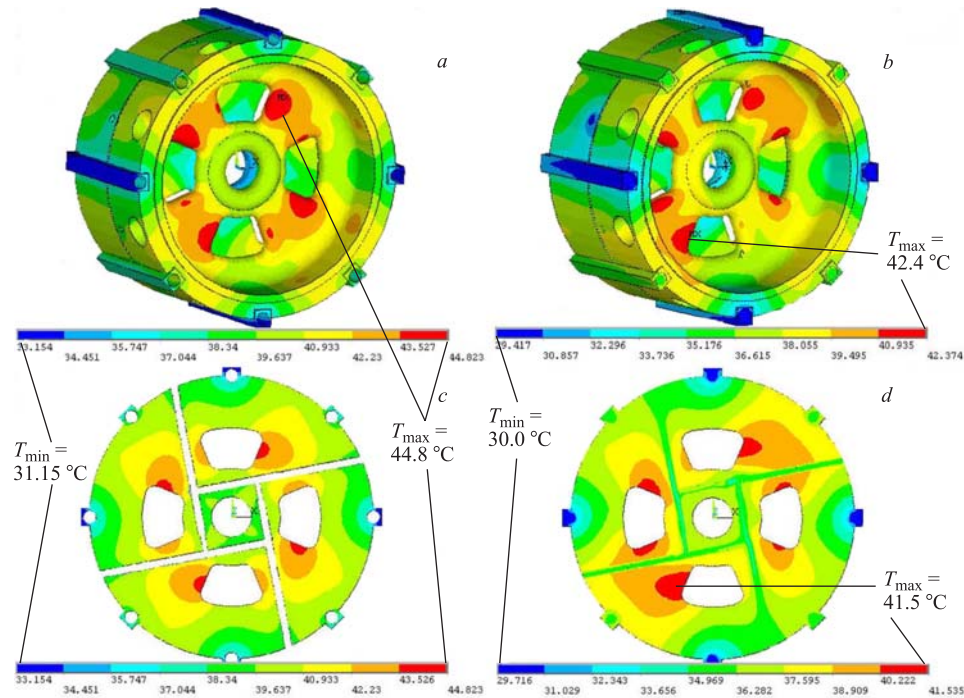


Fig. 5. Temperature distributions in BC CDS cell calculated in engineering (*a*) and conjugated (*b*) approaches. Temperature distributions in the plane of cooling channels (*c*, *d*)

CDS structure has a sufficient reserve in cooling capability. Additional nonuniform pulsed heat load ~ 15 kW due to particle losses in the first capture section [2] is not a problem for average structure heating [6]. Nonuniform (along the section) cell frequencies shift due to particle losses will not cause field distribution distortion — the structure is compensated.

4. PPA BEAM LOADING

For ILC beam specification [2] time interval between positron bunches (~ 300 ns) is not negligibly small in comparison with accelerating structure time constant (rise time for SW or filling time for TW options). Beam loading effect has particularities both from stored energy acceleration regime and the continuous beam loading one. Before beam separation, PPA beam pulse consists of several e^+ and e^- bunches, Fig. 6, *a*. Useful positrons take part in the first e^+ bunch. To ensure $2 \cdot 10^{10} e^+$ at the ILC interaction point, there should be total number $\approx 10^{11}$ particles, both e^+ and e^- , in PPA beam pulse before separation, with total charge ≈ 16 nC. Such a beam pulse takes $\approx 3\%$ of energy, stored in the structure and leads to electric field decreasing. Field recovery pattern between beam pulses is quite different for SW and TW options. For TW structure with very low group velocity [7], several (up to 11) steps at the field distribution along the structure will exist. For compensated in SW structure time dependence of «saw-tooth» field amplitude pattern, Fig. 6, *b*, is realized. Both for SW and TW structures, additional RF power is required to compensate beam loading effect. Even with higher RF power increase for beam loading compensation, total RF power, required for desired e^+ energy gain, is lower for SW option. For PPA output e^+ energy ≈ 400 MeV SW option saves two RF channels. From the point of RF power saving, beam separation in PPA is preferable as early as it is reasonable from e^+ dynamics conditions.

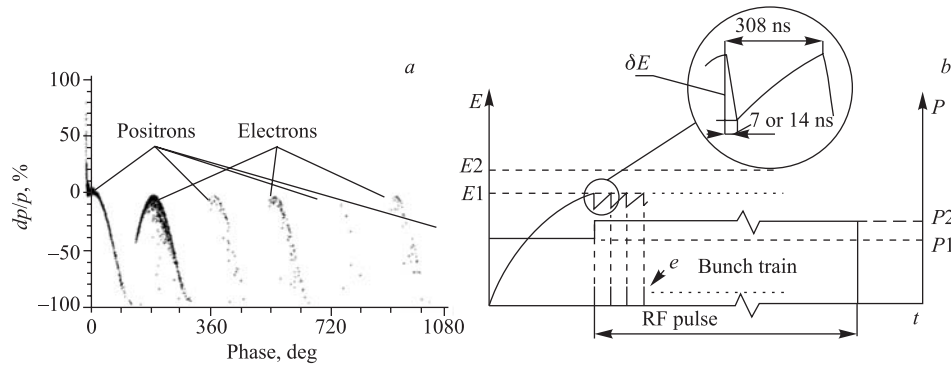


Fig. 6. Beam pulse structure (*a*) and field amplitude envelope (*b*) in PPA part before beam separation

In more detail PPA beam loading is considered in [9].

REFERENCES

1. Conceptual Design of a Positron Injector for the TESLA Linear Collider/Eds. K. Floettmann, V. Paramonov. TESLA 99-14, TESLA 2000-12. Hamburg: DESY, 1999; 2000.
2. ILC Conceptual Design Report. <http://www.linearcollider.org>

3. *Moiseev V. et al.* Comparison of SW and TW Operations for a Positron Pre-Accelerator in the TESLA Linear Collider // Proc. of EPAC2000. 2000. P. 842.
4. *Paramonov V. V.* The Cut Disk Structure for High Energy Linacs // Proc. of 1997 PAC. 1998. V. 3. P. 2962.
5. *Brusova N. I. et al.* Design Parameters of the Normal Conducting Booster Cavity for the PITZ-2 Test Stand // Proc. of LINAC 2004. 2004. P. 204.
6. *Krasilnikov M. et al.* The PITZ Booster Cavity — a Prototype for the ILC Positron Injector Cavities // Proc. of PAC 2005. 2005. P. 1030.
7. *Wang J. W. et al.* Studies of Room Temperature Structures for the ILC Positron Source // Ibid. P. 2827.
8. *Paramonov V. V., Skasyrskaya A. K.* Pulsed RF Heating Simulations in Normal Conducting L-Band Cavities. TESLA-FEL Report 2007-04. Hamburg: DESY, 2007.
9. *Paramonov V. V., Floetmann K.* Beam-Loading Effect in the Normal-Conducting ILC Positron Source Pre-Accelerator // Proc. of 2006 LINAC. 2006. P. 355.